ADVANCED FUNCTIONAL MATERIALS
www.afm-journal.de

Fabrication of Responsive, Softening Neural Interfaces

*Taylor Ware, Dustin Simon, David E. Arreaga-Salas, Jonathan Reeder, Robert Rennaker, Edward W. Keefer, and Walter Voit**

A novel processing method is described using photolithography to pattern thin-film flexible electronics on shape memory polymer substrates with mechanical properties tailored to improve biocompatability and enhance adhesion between the polymer substrate and metal layers. Standard semiconductor wafer processing techniques are adapted to enable robust device design onto a variety of softening substrates with tunable moduli. The resulting devices are stiff enough (shear modulus of ≈700 MPa) to assist with device implantation and then soften in vivo (≈300 kPa) approaching the modulus of brain tissue (≈10 kPa) within 24 h. Acute in vivo studies demonstrate that these materials are capable of recording neural activity. Softening multi-electrode arrays offer a highly customizable interface, which can be optimized to improve biocompatibility, enabling the development of robust, reliable neural electrodes for neural engineering and neuroscience.

1. Introduction

Cortical neural interfaces provide a communication platform for direct interaction with the nervous system.[1–4] Communication with the central nervous system has enabled treatment of numerous conditions such as epilepsy and depression, control of prosthetic devices and the advancement of the field of neuroscience.[5–7] However, devices designed to record extracellular neural activity generally fail within one year of implantation.[8–10] This failure has been widely attributed to gliosis, the chronic reactive biological response to the foreign probe, which leads to death of neurons and encapsulation of the implant resulting in a loss in the signal-to-noise-ratio over time.[11–15] A number of factors contribute to the timeframe and extent of the observed gliosis: size, stiffness, surface chemistry, insertion procedure and mechanical constraints provided by electrical contacts have been shown to have a direct effect on glial scarring.[16–18] The focus of this work is to minimize device stiffness, but each parameter must be considered in device development.

Neural interfaces are typically made of silicon microneedles, planar electrodes or metal microwires.[19] The extreme mechanical mismatch between these devices (commonly tungsten or silicon) is strongly linked to the extensive gliosis and reduction in signal quality over time.[8,9] Recently much research has focused on the design, manufacture and implantation of flexible probes made from polymers, such as polyimides or Parylene-C, with thin-film conductors defined by photolithography; these devices have a reduced mechanical mismatch between neural tissue and the implants.[9,10,20–27] Polymer probes are stiff enough for implantation into the cortex directly or with the aid of an insertion tool, depending on geometry.[25,28] These polymers are still, however, 5 or 6 orders of magnitude stiffer than the surrounding neural tissue. Softening neural interfaces have been demonstrated utilizing the swelling of a nanocomposite polymer film.[29–31] Combining advances in polymer-based probes and shape memory polymers (SMPs) will allow for the further development of devices that are stiff enough for insertion, but undergo orders-of-magnitude reduction of stiffness following insertion.

SMPs are a class of mechanically active materials used to store a metastable shape and return to a globally stable shape upon activation by a stimulus, such as temperature, humidity, light or a combination of these stimuli.[32–34] In thermally active SMPs, recovery is induced by heating the polymer through a transition, such as crystalline melting or a glass transition, leading to a considerable drop in modulus.[35] SMP activation by humidity is a variation of thermal activation, where the drop in modulus is triggered by plasticization of the polymer leading to thermal activation at a lower temperature.[36] Many thermally activated SMP biomedical devices have been proposed including cortical probes that self-insert upon recovery of the device.[37,38] Cortical probes fabricated on an SMP specifically tuned to soften after insertion into the brain have not been previously

T. Ware, D. Simon, D. E. Arreaga-Salas, Prof. W. Voit
Department of Materials Science and Engineering
The University of Texas at Dallas
800 West Campbell RD,
Mailstop RL 10, Richardson, TX 75080, USA
E-mail: walter.voit@utdallas.edu
J. Reeder, Prof. W. Voit
Department of Mechanical Engineering
The University of Texas at Dallas
800 West Campbell RD,
Mailstop RL 10, Richardson, TX 75080, USA
R. L. Rennaker II
School of Behavioral and Brain Sciences
Erik Jonnson School of Engineering
The University of Texas at Dallas
800 West Campbell RD,
Mailstop RL 10, Richardson, TX 75080, USA
E. W. Keefer
Plexon Inc.,
6500 Greenville Ave., Suite 730, Dallas, TX 75206, USA

DOI: 10.1002/adfm.201200200

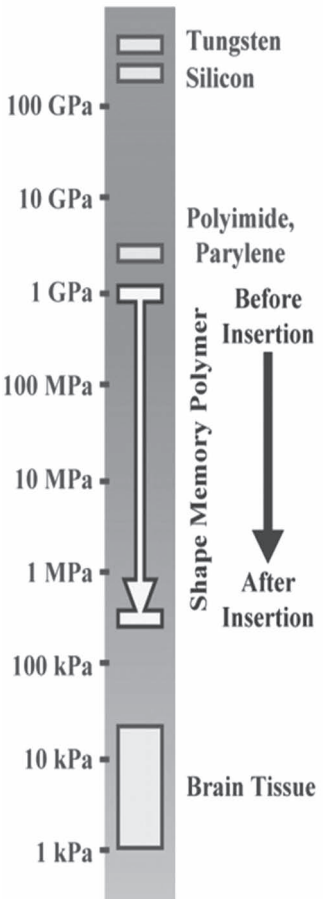

Figure 1. Schematic demonstrating the modulus of materials utilized in neural interfaces and the modulus range of the polymer system studied herein.

discussed in the literature. These softening probes behave similarly to current generation flexible probes during insertion and soften to behave as an elastomer after insertion. This concept is demonstrated schematically in **Figure 1**. Research in flexible electronics has produced neural interfaces on flexible substrates such as, Parylene-C, various polyimides and other engineering thermoplastics, and soft, elastomeric substrates.[39–41] Processing by photolithography on shape memory polymer substrates that demonstrate a dramatic change, from flexible to soft, triggered by physiological conditions has not been studied extensively. Such a process is necessary for the patterning of microelectrodes and must be understood to enable development of reliable high density interfaces. Furthermore, coupling SMP substrates and these design paradigms with the proposed process to enhance adhesion builds a foundation upon which a variety of robust, self-softening, flexible biotechnology devices can be fabricated.

In this work, a thermally and water sensitive SMP system is synthesized and characterized based on commercially-available acrylate monomers. A modular transfer-by-polymerization process to fabricate highly reproducible, robust electrodes for interfacing with cortical tissue on these physiologically active SMPs is developed. All features are produced with photolithography allowing high electrode count with small and precise features on a variety of different substrates. This process is designed to enhance chemical and mechanical interactions between a lithographically defined Au/Cr electrode and the tailored polymer system to improve metal-polymer adhesion. (Meth)acrylate polymers inherently contain both hydrophobic and hydrophilic components; this is utilized to tailor thermo-mechanical properties in physiological conditions and the metal-polymer interaction. While in the past some SMP-based electrodes have been fabricated using other transfer processes, to the authors' knowledge this is the first example in the literature of utilizing the chemical structure of the SMP to provide controlled interaction of lithographically defined electrodes.[42,43] A comparison between the transfer-by-polymerization process and a more traditional approach of metal deposition directly onto a premade polymer substrate is provided. Cortical probes containing 8 gold recording electrodes and a large ground electrode are implanted in the cortex of a laboratory rat and used for acute recording.

2. Results

Two inextricably linked goals of this work demonstrate aspects of the transfer-by-polymerization process: 1) synthesize a physiological responsive substrate to enable neural recording devices that are rigid during processing and insertion and soft after implantation and 2) fabricate and incorporate high-density electrodes onto these substrates in a way that fully utilizes the available functional groups in the underlying substrate to provide a robust bond between the deposited materials and the polymers. Process engineering for devices with tunable substrate properties requires simultaneous consideration of the substrate synthesis, device fabrication, application requirements and environment. A substrate designed to soften in physiological conditions with the onset of the dry glass transition above 45 °C, was selected to allow electrode definition using photolithography. Processing requirements are further explained in the Section 3.

2.1. Synthesis of Dynamically Softening-Substrate

A system comprised of monomers methyl acrylate (MA) and isobornyl acrylate (IBoA) crosslinked with 1 wt% poly(ethylene glycol) diacrylate was copolymerized in varying concentrations to control the glass transition temperature (T_g) and maintain hydrophobicity of the resulting substrates.[44] The ratio of MA and IBoA was tuned such that the onset of the glass transition would be 60 °C. Additionally, a set of other comonomers was screened to increase the hydrophilic nature of the network; 10 wt% comonomer was chosen to evaluate the efficacy of each potential new substrate at softening in physiological conditions. 2-hydroxyethyl acrylate (2HEA), 2-hydroxyethyl methacrylate (2HEMA), acrylic acid (AA) and mono-2-(Methacryloyloxy)ethyl succinate (succinate) each contain hydroxyl groups or carboxylic acids. These groups when incorporated into acrylic copolymers have been shown to increase the hydrophilic behavior in the system. The T_g of each composition was tuned according to

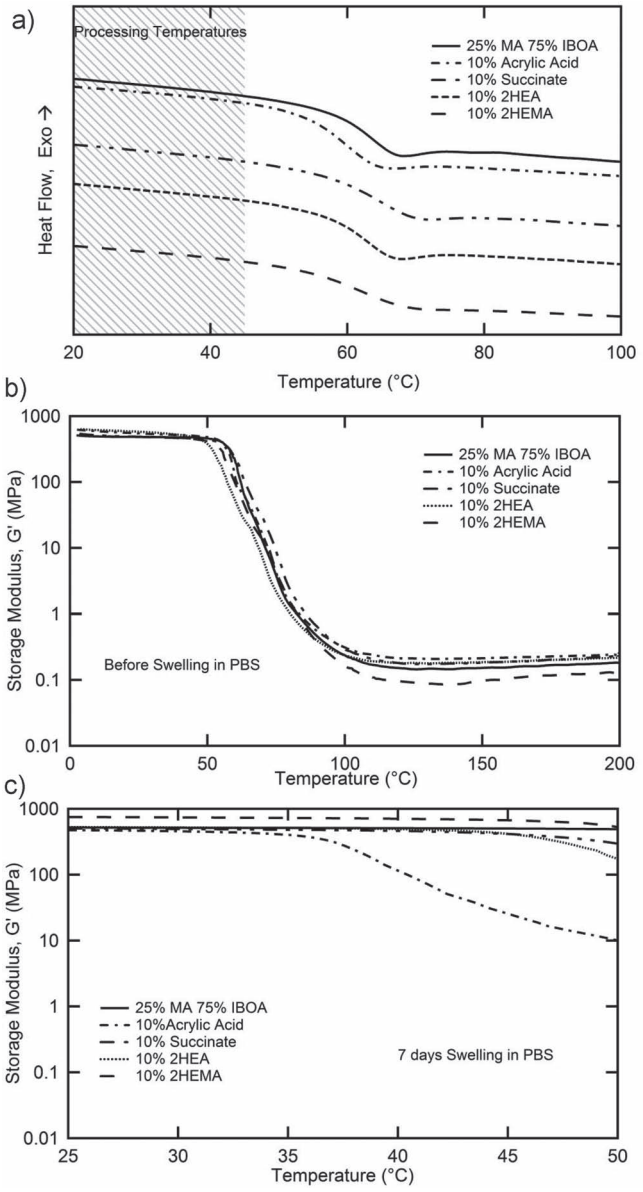

Figure 2. a) DSC of several compositions containing different hydrophilic monomers. The processing range utilized in device production is highlighted. b) DMA of the same compositions shown in (a) before swelling. c) Post-swelling DMA of the compositions characterized in (a,b) with considerable softening shown for the sample containing acrylic acid.

the effect of each comonomers to be equal to that of the base composition 25 wt% MA, 75 wt% IBoA. Differential scanning calorimetry (DSC) and dynamic mechanical analysis (DMA) of the five selected samples, while dry, is shown in **Figure 2**a,b. Each network exhibits largely similar thermomechanical properties with the T_g of each sample by both DMA and DSC varying by less than 5 °C. It should be noted that the shear storage modulus at body temperature is very similar for each sample (~700 MPa). These samples were swollen in phosphate buffered saline for 1 week and retested by DMA. Figure 2c indicates that the sample containing 10 wt% acrylic acid (AA) undergoes significant plasticization. Other hydrophilic comonomers did not have the same magnitude of effect as AA. DMA on swollen materials was not performed while the sample was immersed in PBS but immediately after removal.

Due to the enhanced softening effect of substrates copolymerized with AA, further samples were synthesized containing between 10 wt% and 20 wt% AA using a fixed percentage of MA (40 wt%) that positioned the T_g near 60 °C for 10 wt% AA and replacing IBoA with AA directly for samples containing greater than 10 wt%. For dry samples, as shown in **Figure 3**

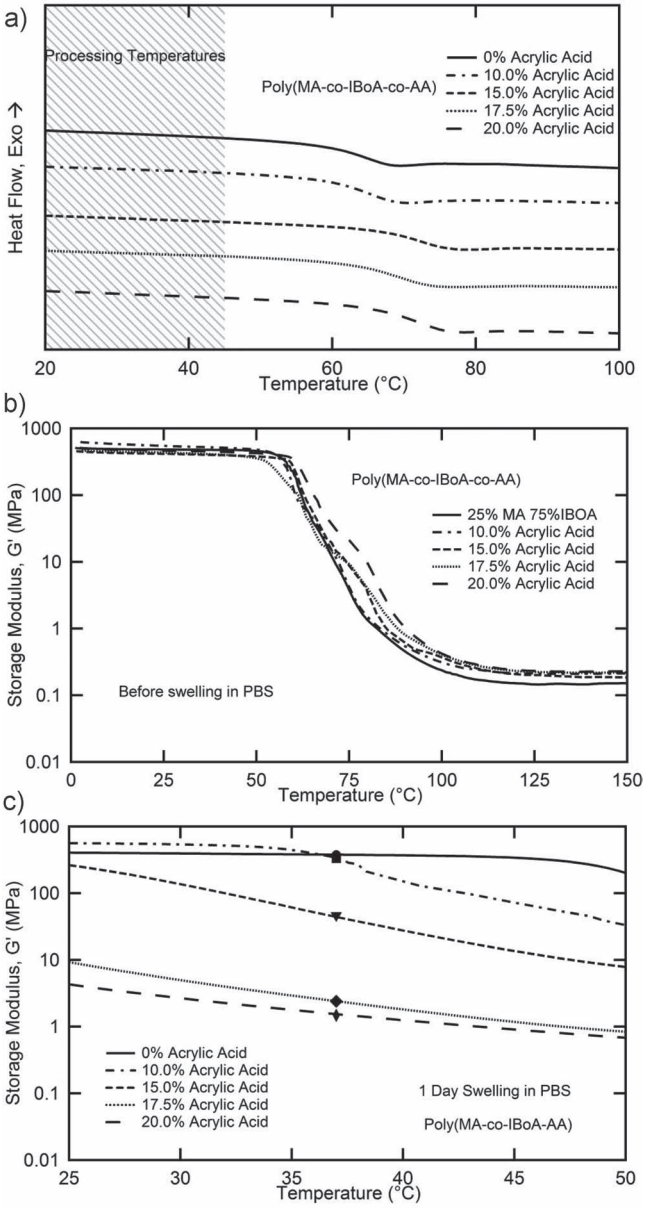

Figure 3. a) DSC of several compositions containing different concentrations of acrylic acid. The processing range utilized in device production is highlighted. b) DMA of the same compositions shown in Figure 2a before swelling. c) 1 day post-swelling DMA of the compositions characterized in (a,b) with considerable softening shown for the sample containing more than 10 wt% acrylic acid. Markers indicate body temperature modulus for each composition.

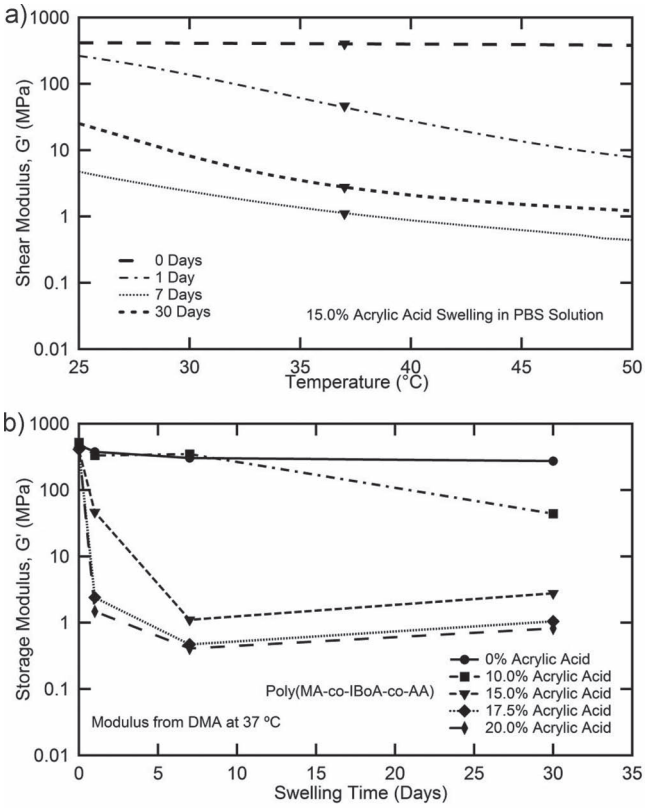

Figure 4. DMA of polymer samples after swelling in PBS solution. a) Modulus as a function of temperature for polymer samples containing 15% acrylic acid after swelling between 0 and 30 days. Markers indicate the body temperature modulus for each time point. b) Body temperature modulus for five selected compositions over one month of swelling.

a, T_g by DSC slightly increases with AA content. DMA, in Figure 3b, is consistent with the DSC and shows the modulus drop associated with T_g is largely the same for each composition. Figure 3c shows the effect of 1 day immersion in PBS on the 4 AA-containing samples as well as the control 25 wt% MA, 75 wt% IBoA sample. No significant drop in modulus at physiological temperature (indicated by markers on each curve) is observed over 1 day for the control or 10 wt% AA sample. Polymerizing 15 wt% AA into the MA-IBoA copolymers yields a drop in modulus of approximately 1 order of magnitude upon immersion in PBS. Incorporating 17.5 wt% and 20 wt% AA monomers each yields a drop in modulus of approximately 2 orders of magnitude.

Figure 4a shows the progression of the modulus drop of the 15 wt% AA sample over 1 month of immersion in PBS. Immersion causes a decrease in modulus of larger than 2 orders of magnitude over 1 week and a slight increase in modulus at 1 month. Figure 4b shows the evolution of the body temperature modulus for the control and 4 AA-containing samples over 1 month. For samples containing greater than 10 wt% AA, each sample softens significantly over 1 week and shows slight stiffening between 1 week and month. The control sample softens very little over this time period, and the 10 wt% AA sample softens approximately 1 order of magnitude. The control substrate and the 4 AA-containing substrates were chosen for device fabrication and process characterization.

2.2. Fabrication of Electrodes: Transfer-by-Polymerization

Photolithography often requires and exposes the substrate to organic solvents, water, heat, vacuum, bases and acids. It also requires that the adhesion between thin films and substrates be sufficient for processing, and that the substrate not deform sufficiently, by mechanical means or from thermal expansion, to crack the often fragile thin films. The polymer substrates used in this study are sensitive to many of these conditions and process control is crucial. To overcome these challenges a transfer-by-polymerization is described. Parylene-C was deposited on a large clean microscope slide to serve as a sacrificial substrate. On this sacrificial substrate, gold and then a chromium adhesion layer were deposited and patterned using electron-beam deposition, photolithography and subsequent wet etching. **Figure 5**a shows, schematically and with SEM, a portion of the substrate in this step. Using this glass slide as the bottom of a mold consisting of another clean glass slide and a spacer of the desired thickness, a mold is constructed. The mold is then filled with the monomer solution and polymerized with 365 nm UV light. After polymerization, the Parylene-C sacrificial layer and electrodes are transferred to the SMP

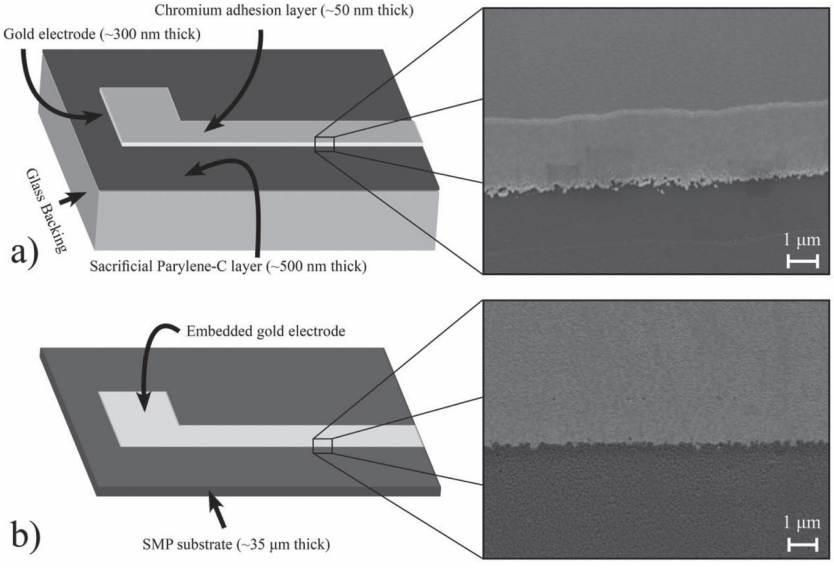

Figure 5. Process schematics (left) and images (right) demonstrating the utilized transfer-by-polymerization process. Substrate prepared for transfer of patterned devices from sacrificial to final substrate (top) schematic. Devices after synthesis of the final substrate and removal of the sacrificial substrate (bottom).

Table 1. ASTM D3359 swelling and adhesion tape test results comparing the transfer-by-polymerization process and direct metal deposition.

Composition	Swelling [%]	Transfer-by-Polymerization		Direct Metal Deposition	
		Dry	10 days swelling	Dry	10 days swelling
25.0% MA 75.0% IBOA	3.4 ±0.4	5B	5B	4B	3B
10.0% Acrylic Acid	15.4 ± 0.4	5B	5B	3B	0B
15.0% Acrylic Acid	195.5 ± 13.8	5B	5B	5B	0B
17.5% Acrylic Acid	216.5 ± 12.5	5B	5B	4B	0B
20.0% Acrylic Acid	326.1 ± 9.7	5B	5B	2B	0B
25.0% MA 75.0% IBOA*	–	0B	0B	0B	0B

substrate. This is enabled by the poor adhesion of Parylene-C to glass. The device is flipped over, removed from the mold and the sacrificial layer of Parylene-C is removed by reactive ion etching (RIE) with oxygen plasma. The sample in this stage is shown in Figure 5b. It should be noted that the gold is now exposed and the top plane of the electrode is shared with the surface of the polymer. The sample is then recoated with a new layer of Parylene-C to insulate the devices with a pinhole free coating. Using photolithography, recording sites and electrical contacts are patterned and opened using RIE.

Metal film adhesion to the SMP substrate is measured by a tape test, described in ASTM D3359. For this test an unpatterned metal film is either transferred-by-polymerization onto the SMP substrate or fabricated through metal evaporation directly onto a premade substrate. The level of adhesion to the substrate is quantified by the amount of delamination witnessed, with 5B indicating no delamination and 0B indicating large-scale delamination. As seen in **Table 1**, all samples with a chromium adhesion layer prepared by the process showed no delamination both as dry samples and after swelling in PBS for 10 days. Direct metal deposition led to moderate to good adhesion in the dry state, but nearly complete delamination after swelling for 10 days for samples containing AA. Very poor adhesion was observed if no chromium adhesion layer was used with the polyacrylate systems regardless of method. The level of swelling increases with AA content

Surface roughness of the synthesized polymer was measured by atomic force microscopy (AFM). Topographical images for two compositions for each processing method are shown in **Figure 6**. Images are of the polymer surface after transfer-by-polymerization or deposition and subsequent wet etching of the metal. The transfer-by-polymerization procedure provides surfaces with ~1.5–2 times less surface roughness as quantified by AFM. It should be noted that there is not a statistical difference between samples processed with the same method for the compositions tested.

Samples prepared through the same method as those characterized with AFM were characterized with X-ray photoelectron spectroscopy (XPS). The carbon region of the spectra with peak deconvolutions is shown in **Figure 7**. Samples prepared by direct metal deposition do not show large differences in measured spectra between the two samples. Samples prepared through transfer-by-polymerization, however, reflect the more polar nature of the 20 wt% AA containing sample with increased carbon–oxygen interactions. This is noted by the appearance of peaks at higher bonding energies as compared to the carbon-carbon peak. Peaks that could be assigned based on literature values of the distance from the C-C peak are labeled.

Cortical probes were not successfully fabricated using direct metal deposition due to challenges posed during processing. **Figure 8**a,b shows two optical micrographs of the cortical probes fabricated using the transfer-by-polymerization process depicting the entire device (Figure 8b) and the recording electrodes (Figure 8a). Cortical probes have been fabricated using all four AA-containing compositions as well as the control composition containing only MA and IBoA. Acute recording data are presented in Figure 8c,d with the recording of repetitive single-unit action potentials from the rat somatosensory cortex. Signal-to-noise ratios exceeding 5 to 1 were achieved.

3. Discussion

Neural interfaces have traditionally been made of materials with moduli 5 to 9 orders of magnitude stiffer than neural tissue. In this work, SMP cortical recording electrodes fabricated and inserted in the high modulus state soften three orders of magnitude due to a combination of thermal stimuli and plasticization by water uptake. Demonstration of a modular

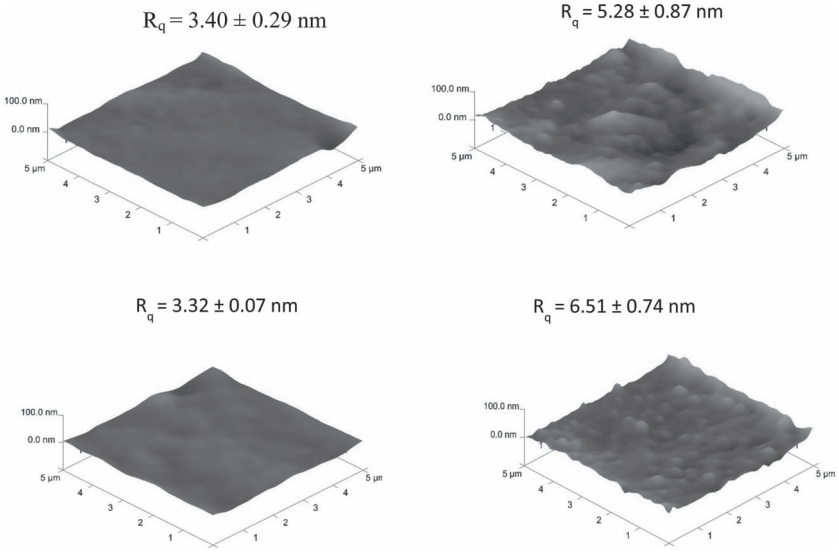

Figure 6. AFM of samples made by transfer-by-polymerization (left) and direct deposition (right). Two compositions are presented 25% methyl acrylate-75% isobornyl acrylate (top) and 20% acrylic acid (bottom).

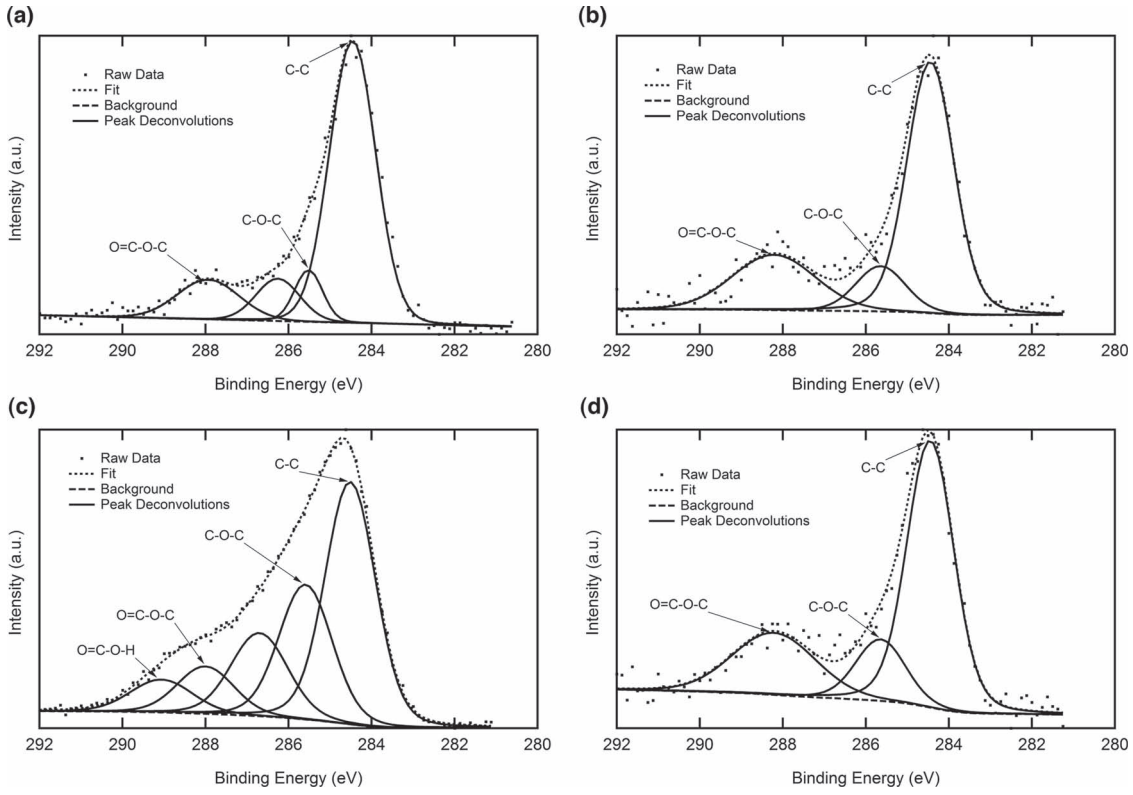

Figure 7. XPS of samples prepared by transfer-by-polymerization (left) and direct deposition (right) both of which subsequently had the metal etched. Only the carbon region of the spectrum is presented. Two compositions are presented 25% methyl acrylate-75% isobornyl acrylate (top) and 20% acrylic acid (bottom).

transfer-by-polymerization process for the manufacture of SMP-based flexible electronic devices requires control over electrode patterning, substrate synthesis, subsequent lithography and final device performance. The process developed in this work provides much of this modularity. Conductor patterning is only limited by the constraints of photolithography on the sacrificial substrate. Substrate properties and conductor-polymer interactions are dictated by starting monomer chemistry which can vary widely based on commercially or synthetically available monomers.

Photolithography is used in two distinct processing stages: first, to pattern devices on the initial sacrificial substrates and second, to encapsulate and define recording sites on manufactured devices. The second, device encapsulation and recording site definition by photolithography of Parylene-C, occurs with the physiologically responsive, softening polymer as the substrate. As such, certain basic requirements on substrate properties were established to enable this processing. This stage requires temperature exposure of up to 40 °C, to bake the photoresist, but no more to shift the substrate through its dry T_g during processing. Due to the large difference in coefficient of thermal expansion of polymers above T_g and the thin film metals used in this study, all substrates were kept below dry T_g to prevent cracking of the electrode. A target dry T_g was determined to be 60 °C to provide a safety factor for device fabrication. A system of copolymers containing 10 wt% of different hydrophilic monomers was established with very similar T_g (±3 °C), as shown in Figure 2a,b. This constant T_g allows for identical dry processing conditions for devices irrespective of the selected monomers. Despite the similarity in dry thermomechanical properties, AA-containing polymers showed significant softening in physiological conditions as seen in Figure 2c. While the 10 wt% AA sample begins to soften at 37 °C in PBS, the body temperature modulus is still more than 3 orders of magnitude stiffer than brain tissue. Water-loss does occur during testing, but the utilized method allows for elucidation of trends in thermomechanical properties of these polymers during simulated implantation.

Increasing the concentration of AA, in the monomer solution, yields substrates with a higher degree of plasticization following implantation. The basic condition that the dry substrates must remain in the glassy state below 50 °C was maintained for processing reasons. The T_g as measured by DSC, and shown in Figure 3a, generally increases with AA content. DMA, shown in Figure 3b, indicates the breadth and location of the transition is relatively unaffected by introduction of AA, and that all samples behave in a glassy manner below 50 °C. After 1 day immersion in PBS, a stark contrast between the mechanical responses of the samples can be noted in Figure 3c. The modulus at body temperature decreases strongly with AA content. One day immersion in PBS was insufficient for the modulus of the samples to equilibrate; significant softening continues over the first week shown in Figure 4a,b. Samples containing 15 wt% AA or greater showed slight stiffening over a month after the initial

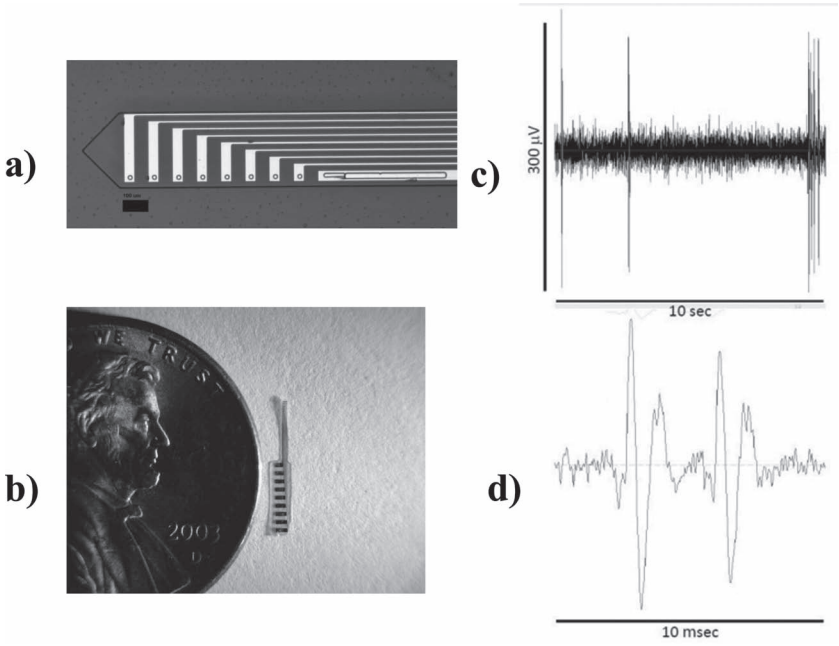

Figure 8. Optical microscopy images of example cortical probes fabricated using the transfer-by-polymerization process. Cortical probe with 8 recording channels and a ground fabricated and insulated with patterned Parylene-C (a). Cortical probe shown for perspective next to an American penny (b). Recording sites are at the top of the device and electrical contacts are at the bottom. Single unit action potential recording from rat somatosensory cortex with SMP-gold electrode array during an acute experiment (c). Signals with signal-to-noise ratios in excess of 5:1 were easily obtained. Close up of single unit repetitive firing shows amplitude accommodation typical of excitatory neurons (d).

desired precipitous drop in modulus. This delayed stiffening effect (of approx. 1 MPa) has been reported previously in acrylate copolymers similar to the polymers studied here.[45] The exhibited physiological modulus is due to both substrate plasticization by PBS and the temperature. The extent of substrate swelling will have a direct effect on the electrical properties of fabricated devices. There is an applied strain to the thin film metals induced by the change in volume of the substrate that can lead to electrode failure. Devices fabricated on the control substrate (25 wt% MA, 75 wt% IBoA) showed nominal change in resistance for a period up to 3 months, while devices fabricated on substrates with 20% AA lost electrical continuity after 24 hours due to the large change in volume. Future work will study how electrical properties change with the swelling profile of the substrate and how mechanical design can improve the recording fidelity of devices over time.

The second goal of this study is device fabrication based on the responsive substrate and not despite it. While substrate softening and compatibility with further processing are important factors in the determination of the basic viability of the studied system, understanding the interface between the metallic electrode and polymeric substrate is necessary to understand device durability. The specific parameter of interest is the adhesion of the electrode to the substrate. Polymer substrates are often chemically modified after polymerization to introduce oxygen-containing functional groups to increase adhesion.[46,47] When a polymer is polymerized directly onto a surface as in the described transfer process, the high mobility in the monomeric state allows for formation of the most favorable interaction, both mechanically and chemically, with the electrode. The transfer-by-polymerization process allows for this interaction to form and then be locked into place by virtue of the polymerization. The chosen monomers already contain ether, ester and carboxylic acid functionalities with a high tendency of adhesion to the oxidized chromium adhesion layer as compared to the carbon-carbon polymer chains. In addition to the tendency for chromium to adhere to polymers with polar functionalities on the surface, it also adheres well to gold. The results in Table 1 indicate the effects of these factors on the adhesion of an unpatterned metal film were substantial. All samples processed by the transfer-by-polymerization method achieved the highest score provided by the ASTM both in the dry state and after immersion in PBS for 10 days. Samples processed using direct metal deposition exhibited moderate adhesion in the dry state, but all AA-containing samples exhibited near-complete delamination after PBS immersion. To provide evidence into the chemical mechanism of this enhanced adhesion chemical and elemental information from the polymer surface is provided in Figure 7. The increased tendency for these functional groups to migrate to the surface when polymerized directly on the adhesion layer, as compared to direct metal deposition, is measured by XPS. AA also serves to increase the polarity, distance away from the C-C peak, and quantity of the functional groups found at the surface as compared to the control sample. Mechanical adhesion is provided by the use of a low viscosity liquid monomer, which allows the surface of the polymer to form in intimate mechanical contact with the adhesion layer. AFM in Figure 6 shows that polymer polymerized on the metal showed approximately half the surface roughness as compared to the pre-polymerized substrate. The premade polymer was made on a glass slide with low surface roughness, $R_q < 1$ nm, but this polymer must be removed and then have metal deposited which causes localized heating. In this process the polymer surface is deformed and may pick up unwanted material, decreasing the contact area with the evaporated film. Efforts were made to maintain the surface of the pre-polymerized substrate clean, but thorough cleaning prior to deposition is not possible without causing swelling as the polymer is susceptible to most organic solvents and water. This is another processing limitation on premade substrates that are water and solvent sensitive.

Cortical recording probes could not be directly tested for adhesion based on ASTM D3359. Most electrodes based on thin films are made by deposition and patterning on top of a substrate, as is demonstrated on the sacrificial substrate in Figure 5a. Figure 5b shows that after transfer the polymer substrate and electrode share the same top plane. This increases the path tortuosity of a delaminating crack and should also improve observed device-substrate adhesion.

Cortical recording probes were fabricated using the described transfer-by-polymerization process, with a minimum feature size of 15 μm. This feature size could be markedly decreased in more advanced generations and is not a fundamental limitation of the process itself. The devices served as functional recording devices on acute timescales. Signal-to-noise ratios above the generally accepted threshold of 5 to 1 were achieved. Successful recording of an excitatory neuron in a rat cortex is demonstrated in Figure 8c,d. While initial investigation has focused on cortical recording devices, a number of other neural biotechnology devices ranging from in vitro multi-electrode arrays to nerve cuff electrodes to cochlear implants are currently being explored utilizing the described process and other processing conditions. Several key challenges remain that limit device implementation. These devices need to be sterilized for implantation; for this work, 254 nm UV light was used for this purpose. However these substrates are strongly affected by isopropanol and cannot withstand autoclave temperatures leading to device disfiguration. Temperatures well above 40 °C are also useful in making reliable, low-resistance electrical contact to the device. Currently research is focused on overcoming these and other limitations using alternate electrode materials, both inorganic and organic, and exploring other polymer systems. These changes can be made readily without reinventing the basic concept of the transfer process as described.

4. Conclusions

Cortical recording electrodes have received much research attention for their ability to revolutionize direct electrical interaction (both stimulation and recording) with the central nervous system. This work utilizes the tailorable significant modulus change of acrylic shape memory polymers that can be activated by physiological conditions. The produced cortical probes soften post-insertion to more closely match the modulus of cortical tissue. Devices are fabricated using a transfer-by-polymerization process that allows for full-photolithographically defined electrodes on temperature and solvent sensitive substrates. Also utilized are the inherently available polar function groups in the chosen system to greatly increase adhesion as compared to traditional methods. This process is modular and will allow for tuning of substrate chemistry and electrode design for future improvements in various nervous system interfaces and in the broader field of flexible and stretchable electronics. Ongoing work seeks to quantify the realized benefit of the softening substrate with immunohistochemistry and extensive electrical recording and fabricate a host of other neural biotechnology devices by this process.

5. Experimental Section

Methyl acrylate (MA), isobornyl acrylate (IBoA), 2-hydroxyethyl acrylate (2HEA), 2-hydroxyethyl methacrylate (2HEMA), acrylic acid (AA), mono-2-(Methacryloyloxy)ethyl succinate (succinate), poly(ethylene glycol)diacrylate (M_n~575), phosphate buffered saline (PBS), and 2,2-dimethoxy-2-phenyl acetophenone (DMPA) were purchased from Sigma Aldrich. All chemicals were used as received without further purification. All processing steps except polymer synthesis were performed in a Class 10,000 cleanroom.

Sacrificial Substrate Preparation: 75 mm × 50 mm glass microscope slides were cleaned by subsequent steps of scrubbing in an Alconox solution, sonication in acetone, sonication in isopropanol and repeated as necessary until free of optically visible unwanted material. 500 nm of Parylene-C was deposited in a SCS Labcoter 2 (SCS Systems).

Metal Electrode Deposition and Patterning: 300 nm of Au and 50 nm of Cr were deposited, at 0.2 nm/min, using electron-beam evaporation without removing the sample from vacuum.. Electrodes were then patterned by standard photolithography and etched using chromium etchant (CR-7S Cyantek Corporation) and gold etchant (AU-5 Cyantek Corporation). For adhesion tests, AFM and XPS films were not patterned. To test direct metal deposition a previously synthesized polymer film (1 mm thick) was coated with 50 nm Cr and 300 nm Au.

Polymer Synthesis and Electrode Transfer-by-Polymerization: The appropriate (meth)acrylate monomers, 1 wt% PEGDA and 0.1 wt% DMPA were mixed. The monomer solution was injected between two glass slides (75 mm × 50 mm) separated by a glass spacer, 1.2 mm or 35 μm thick. Polymerization was performed using a crosslinking chamber with five overhead 365 nm UV bulbs (UVP via Cole-Parmer) for 120 minutes. Device transfer was accomplished by using the sacrificial substrate with patterned electrodes or unpatterned film as the bottom slide for the mold. Due to the comparatively poor adhesion of the Parylene-C to the sacrificial glass slide devices and Parylene were transferred to the SMP substrate. Care was taken to ensure the bottom glass slide remained on the polymer substrate.

Device Insulation and Recording Site Definition: Reactive ion etching with an oxygen plasma (50 W, 100 mTorr, 6 min) was used to remove the sacrificial Parylene-C layer. RIE was performed with a Technics RIE in intervals of 30 s on and 15 s off to prevent significant device heating. Another layer of 500 nm thick Parylene-C was deposited under the same conditions. This layer was patterned using photolithography, while limiting the resist bake temperature to 40 °C. After Parylene-C etching with RIE under the same conditions, residual photoresist (S1813 Shipley) was removed by a flood exposure and developing. Recording sites were approximately 300 μm^2 in area.

Device Definition and Electrical Bonding: Cortical probes were cut from the surrounding polymer sheet using a CO_2 laser. Final shank width was approximately 0.5 mm. Devices were removed from the carrier glass slide by lifting gently with a moistened razor blade. Probes were electrically bonded to a custom printed circuit board using an anisotropic conductive adhesive (Sunray Scientific) based on magnetically alignable particles in a polymer matrix. Devices for implantation were sterilized by exposing to 254 nm UV light for 3 h.

Dynamic Mechanical Analysis: DMA was performed on a Mettler Toledo DMA 861e/SDTA. Samples were cut into cylinders approximately ~1 mm thick and ~3 mm in diameter. The mode of deformation was shear, and strain was limited to a maximum of 0.3%. Samples were tested at a heating rate of 2 °C/min. A multiplexed frequency mode was run on all samples in which 1, 2, 5 and 10 Hz deformation occurs simultaneously; the frequency of deformation shown is 1 Hz. Tests were conducted in a nitrogen atmosphere. DMA on swollen samples was performed by immediately removing a swollen sample and testing in shear parallel-plate configuration. In this configuration approximately 70% of the surface area of the sample is in contact with the clamping assembly slowing evaporation. This method was selected as it is appropriate for both swollen samples and for explanted samples. Comparison of in vitro and in vivo immersed samples is an area of continuing work. While this method does permit some water loss during testing it provides a conservative estimate of the modulus drop of the polymer in physiological conditions. It should be noted that all samples that were swollen were chosen to be appropriately sized for mechanical testing (~1 mm thick) and are not representative of the dimensions of a cortical probe (~35 μm thick). T_g by DMA is denoted as the peak of tan δ. Each composition was tested twice. The value of the y-intersect for all DMA data presented in this work was chosen to be 10 kPa, approximately the modulus of brain tissue, to maintain the awareness of the reader to the target modulus for the lowest mechanical mismatch.

Differential Scanning Calorimetry: DSC was performed on a Mettler Toledo DSC 1 with an intracooler option. Samples were heated from room temperature to 100 °C, cooled to –50 °C, and subsequently heated to 200 °C. Data shown are of only the second heating ramp. All heating and cooling rates were fixed at 10 °C/min. Tests were conducted in a nitrogen atmosphere. T_g by DSC is denoted as the midpoint of the transition.

X-Ray Photoelectron Spectroscopy: XPS measurements were done on a PHI 5800 spectrometer equipped with an Al Kα monochromated X-ray source. A take-off angle of 90° from the surface was employed. Spectra were recorded with 29.35 eV pass energy, at 0.125 ev/step. The peak locations were corrected on the basis of the C-C (1s) binding energy of 284.5 eV. XPS peak assignments were made based on detailed, self-consistent curve fitting of the recorded spectra using Voigt line shapes in conjunction with a Shirley background subtraction.[48]

Atomic Force Microscopy: Atomic force microscopy was performed in a Veeco, Model 3100 Dimension V Atomic Probe Microscope in tapping mode. An area of 25 μm^2 was scanned at a rate of 1 Hz with a 1 Ohm Si probe with f_0 = 320-359 kHz and k = 12-103 N/m. Three measurements were made per sample.

Scanning Electron Microscopy: Scanning electron microscopy was performed in a ZEISS SUPRA-40. Samples were sputtered with gold to reduce charging effect. Images were captured in a 52° angle; at a working distance and electron high tension of 11 mm and 7 KeV respectively.

Adhesion Testing: Adhesion testing was performed in accordance with ASTM D3359. A crosshatch pattern was scored through the thin metal film to the substrate. A pressure-sensitive tape (SEMicro CHT) was applied to the area of the crosshatch, formed by six parallel cuts and six perpendicular cuts (1 mm dimension squares). The tape was removed quickly at an angle close to 180°. The level of adhesion was quantified by the percentage of the remaining metal coating on the polymer substrate. The scale defined by the standard is: 5B- 0% of coating removed, 4B- Less than 5% removed, 3B–5- 15% removed, 2B- 15-35% removed, 1B-35-65% removed, 0B- Greater than 65% removed.

Acute Neural Recording: Rats were anaesthetized by IP injection, heads fixed in a stereotaxic frame, and the somatosensory cortex exposed. Electrodes were lowered under micromanipulator control until neural activity was evident on an oscilloscope, then electrodes were inserted a further 800 µm. Electrodes rested undisturbed for 5 min, then spontaneous neural activity was recorded with a 16-channel Recording System (Plexon). All experimental procedures were performed in accordance with the National Institutes of Health Guide for the Care and Use of Laboratory Animals, and approved by the UTSW Institutional Animal Care and Use Committee.

Acknowledgements

This material is based partially based upon work supported by the National Science Foundation Graduate Research Fellowship under Grant No.2011113646, the NSF Partnerships for Innovation under Grant No.1114211 and by NIH-NINDS under Grant No.R01 NS062065-02.

Received: January 21, 2012
Revised: March 26, 2012
Published online: May 2, 2012

[1] P. R. Kennedy, R. A. E. Bakay, M. M. Moore, K. Adams, J. Goldwaithe, *IEEE Trans. Rehabil. Eng.* **2000**, *8*, 198.
[2] N. Birbaumer, *Psychophysiology* **2006**, *43*, 517.
[3] T. Stieglitz, *Poiesis Praxis: Int. J. Technol. Assess. Ethics Sci.* **2006**, *4*, 95.
[4] A. B. Schwartz, X. T. Cui, D. J. Weber, D. W. Moran, *Neuron* **2006**, *52*, 205.
[5] S. Musallam, B. Corneil, B. Greger, H. Scherberger, R. Andersen, *Science* **2004**, *305*, 258.
[6] R. Andersen, J. Burdick, S. Musallam, B. Pesaran, J. Cham, *Trends Cognit. Sci.* **2004**, *8*, 486.
[7] J. Harris, A. Hess, S. Rowan, C. Weder, C. Zorman, D. Tyler, J. Capadona, *J. Neural Eng.* **2011**, *8*, 046010.
[8] V. Polikov, P. Tresco, W. Reichert, *J. Neurosci. Methods* **2005**, *148*, 1.
[9] A. Mercanzini, K. Cheung, D. L. Buhl, M. Boers, A. Maillard, P. Colin, J. C. Bensadoun, A. Bertsch, P. Renaud, *Sens. Actuators A* **2008**, *143*, 90.
[10] P. Rousche, D. Pellinen, D. Pivin, J. Williams, R. Vetter, D. Kirke, *IEEE Trans. Biomed. Eng.* **2001**, *48*, 361.
[11] P. Stice, J. Muthuswamy, *J. Neural Eng.* **2009**, *6*, 046004.
[12] S. Levesque, B. Wilson, V. Gregoria, L. B. Thorpe, S. Dallas, V. S. Polikov, J. S. Hong, M. L. Block, *Brain* **2010**, *133*, 808.
[13] E. Azemi, C. F. Lagenaur, X. T. Cui, *Biomaterials* **2011**, *32*, 681.
[14] X. Liu, D. B. McCreery, R. R. Carter, L. A. Bullara, T. G. H. Yuen, W. F. Agnew, *IEEE Trans. Rehabil. Eng.* **1999**, *7*, 315.
[15] P. Rohatgi, N. B. Langhals, D. R. Kipke, P. G. Patil, *Neurosurg. Focus* **2009**, *27*, 8.
[16] V. S. Polikov, M. L. Block, J. M. Fellous, J. S. Hong, W. M. Reichert, *Biomaterials* **2006**, *27*, 5368.
[17] P. C. Georges, W. J. Miller, D. F. Meaney, E. S. Sawyer, P. A. Janmey, *Biophys. J.* **2006**, *90*, 3012.
[18] R. Rennaker, S. Street, A. Ruyle, A. Sloan, *J. Neurosci. Methods* **2005**, *142*, 169.
[19] J. P. Donoghue, *Nat. Neurosci.* **2002**, *5*, 1085.
[20] A. A. Fomani, R. R. Mansour, *Sens. Actuators A* **2011**, *168*, 233.
[21] S. P. Lacour, S. Benmerah, E. Tarte, J. FitzGerald, J. Serra, S. McMahon, J. Fawcett, O. Graudejus, Z. Yu, B. Morrison, *Med. Biol. Eng. Comput.* **2010**, *48*, 945.
[22] E. Patrick, V. Sankar, W. Rowe, S. F. Yen, J. C. Sanchez, T. Nishida, *Proc. 28th Int. Conf. Eng. Med. Biol. Soc.*, Canada **2008.**
[23] E. Patrick, M. Ordonez, N. Alba, J. C. Sanchez, T. Nishida, *Proc. 28th Int. Conf. Eng. Med. Biol. Soc.*, USA **2006**.
[24] C. Pang, J. G. Cham, Z. Nenadic, S. Musallam, Y. C. Tai, J. W. Burdick, R. A. Andersen, *Proc. 27th Int. Conf. Eng. Med. Biol. Soc.*, China **2005**.
[25] D. P. O'Brien, T. R. Nichols, M. G. Allen, *Proc. 14th Int. IEEE Conf. Micro Electro Mechanical Sys.*, Switzerland **2001**.
[26] P. Kohler, C. Linsmeier, J. Thelin, M. Bengtsson, H. Jorntell, M. Garwicz, J. Schouenborg, L. Wallman, *Proc. 31st Int. Conf. IEEE EMBS*, USA **2009**.
[27] N. Akamatsu, T. Suzuki, K. Mabuchi, H. Fujita, B. Kim, S. Takeuchi, *Proc. 25th Int. IEEE EMBS Conf. Neural Eng.*, Mexico **2003**.
[28] T. D. Y. Kozai, D. R. Kipke, *J. Neurosci. Methods* **2009**, *184*, 199.
[29] J. R. Capadona, K. Shanmuganathan, D. J. Tyler, S. J. Rowan, C. Weder, *Science* **2008**, *319*, 1370.
[30] J. P. Harris, A. E. Hess, S. J. Rowan, C. Weder, C. A. Zorman, D. J. Tyler, J. R. Capadona, *J. Neural Eng.* **2011**, *8*, 046010.
[31] J. P. Harris, J. R. Capadona, R. H. Miller, B. C. Healy, K. Shanmuganathan, S. J. Rowan, C. Weder, D. J. Tyler, *J. Neural Eng.* **2011**, *8*, 066011.
[32] W. Voit, T. Ware, R. R. Dasari, P. Smith, L. Danz, D. Simon, S. Barlow, S. R. Marder, K. Gall, *Adv. Funct. Mater.* **2010**, *20*, 162.
[33] D. L. Safranski, K. Gall, *Polymer* **2008**, *49*, 4446.
[34] A. Lendlein, H. Jiang, O. Junger, R. Langer, *Nature* **2005**, *434*, 879.
[35] K. Gall, C. M. Yakacki, Y. Liu, R. Shandas, N. Willett, K. S. Anseth, *J. Biomed. Mater. Res., Part A* **2005**, *73A*, 339.
[36] B. Yang, W. Min Huang, C. Li, J. Hoe Chor, *Eur. Polym. J.* **2005**, *41*, 1123.
[37] A. Lendlein, R. Langer, *Science* **2002**, *296*, 1673.
[38] A. A. Sharp, H. V. Panchawagh, A. Ortega, R. Artale, S. Richardson-Burns, D. S. Finch, K. Gall, R. L. Mahajan, D. Restrepo, *J. Neural Eng.* **2006**, *3*, L23.
[39] T. Suzuki, K. Mabuchi, S. Takeuchi, *Proc. 1st Int. IEEE EMBS Conf. Neural Eng.*, IEEE, Italy **2003**.

[40] J. A. Rogers, T. Someya, Y. Huang, *Science* **2010**, *327*, 1603.
[41] T. Sekitani, Y. Noguchi, K. Hata, T. Fukushima, T. Aida, T. Someya, *Science* **2008**, *321*, 1468.
[42] Z. Yu, Q. Zhang, L. Li, Q. Chen, X. Niu, J. Liu, Q. Pei, *Adv. Mater.* **2011**, *23*, 664.
[43] Z. Yu, X. Niu, Z. Liu, Q. Pei, *Adv. Mater.* DOI: 10.1002/adma.201101986.
[44] W. Voit, T. Ware, K. Gall, *Polymer* **2010**, *51*, 3551.
[45] K. E. Smith, P. Trusty, B. Wan, K. Gall, *Acta Biomater.* **2011**, *7*, 558.
[46] T. Koga, B. Kugler, J. Loewenstein, J. Jerome, M. H. Rafailovich, *J. Appl. Crystallogr.* **2007**, *40*, s684.
[47] W. T. Li, R. B. Charters, B. Luther-Davies, L. Mar, *Appl. Surf. Sci.* **2004**, *233*, 227.
[48] D. A. Shirley, *Phys. Rev. B* **1972**, *5*, 4709.